HHS Public Access

Author manuscript

Circ Res. Author manuscript; available in PMC 2023 August 19.

Published in final edited form as:

Circ Res. 2022 August 19; 131(5): 371–387. doi:10.1161/CIRCRESAHA.121.319955.

Endothelial loss of ETS1 impairs coronary vascular development and leads to ventricular non-compaction

Lu Wang, Ph.D.[1], **Lizhu Lin, Ph.D**[1], **Hui Qi, M.S.**[1], **Ju Chen, Ph.D.**[2], **Paul Grossfeld, M.D.**[1,3]

[1]Division of Cardiology, Department of Pediatrics, UCSD School of Medicine, La Jolla, CA 92093, USA

[2]Department of Medicine, University of California San Diego, La Jolla, CA 92093, USA

[3]Division of Cardiology, Rady Children's Hospital San Diego, San Diego, CA, USA

Abstract

Rationale: Jacobsen syndrome (JBS) is a rare chromosomal disorder caused by deletions in the long arm of human chromosome 11, resulting in multiple developmental defects including congenital heart defects (CHDs). Combined studies in humans and genetically engineered mice implicate that loss of ETS1 is the cause of CHDs in JBS, but the underlying molecular and cellular mechanisms are unknown.

Objective: To determine the role of ETS1 in heart development, specifically its roles in coronary endothelium and endocardium and the mechanisms by which loss of ETS1 causes coronary vascular defects and ventricular non-compaction.

Methods and Results: ETS1 global and endothelial-specific knockout mice were used. Phenotypic assessments, RNA sequencing and chromatin immunoprecipitation analysis were performed together with expression analysis, immunofluorescence and RNAscope *in situ* hybridization to uncover phenotypic and transcriptomic changes in response to loss of ETS1. Loss of ETS1 in endothelial cells causes ventricular non-compaction, reproducing the phenotype arising from global deletion of ETS1. Endothelial-specific deletion of ETS1 decreased the levels of Alk1, Cldn5, Sox18, Robo4, Esm1 and Kdr, six important angiogenesis-relevant genes in endothelial cells, causing a coronary vasculature developmental defect in association with decreased compact zone cardiomyocyte proliferation. Down-regulation of ALK1 expression in endocardium due to the loss of ETS1, along with the up-regulation of TGFβ1 and TGFβ3, occurred with increased TGFBR2/TGFBR1/SMAD2 signaling and increased extracellular matrix (ECM) expression in the trabecular layer, in association with increased trabecular cardiomyocyte proliferation.

Address correspondence to: Dr. Paul Grossfeld, 3020 Children's Way, MC5004, San Diego, California 92123, 858-966-5855 (Office), pgrossfeld@health.ucsd.edu.

DISCLOSURES

The authors have no disclosures.

SUPPLEMENTAL MATERIALS

Expanded Materials & Methods

Online Table I–III

Online Figures I–IX

References 47–51

Conclusions: These results demonstrate the importance of endothelial and endocardial ETS1 in cardiac development. Delineation of the gene regulatory network involving ETS1 in heart development will enhance our understanding of the molecular mechanisms underlying ventricular and coronary vascular developmental defects, and will lead to improved approaches for the treatment of patients with congenital heart disease.

Keywords

non-compaction; coronary vasculature; extracellular matrix; Cardiomyopathy; Animal Models of Human Disease

INTRODUCTION

Congenital heart defects (CHDs) are the most common birth defect in newborn infants, occurring in nearly 1% of the general population.[1] Jacobsen syndrome (JBS, OMIM #147791) is a rare chromosomal disorder caused by deletions in the long arm of human chromosome 11, resulting in multiple developmental defects including CHDs.[2] More than 50% of people with JBS have hemodynamically significant CHDs requiring medical therapy and/or surgical intervention.[3] The genetic pathways required for normal development of the ventricular myocardium are complex, involving signaling pathways between the endocardium and/or coronary endothelium and the developing ventricular myocardium.[4–7] This is further complicated by distinct pathways involved in the development of the trabecular layer and the compact zone for normal ventricular development. Perturbation of either or both of these pathways underlies some forms of cardiomyopathy, e.g. left ventricular non-compaction, and may have a critical role in the pathogenesis of hypoplastic left heart syndrome (HLHS).[8–10]

Although there are numerous genetically engineered mouse models for CHDs, only a small number of these genes are currently associated with CHDs in humans.[1] Combined studies in humans and genetically engineered mice implicate the loss of the ETS1 transcription factor as the cause of CHDs and several other congenital defects in JBS.[11–13] ETS1 is a member of the E26 Transformation Specific (ETS) family of transcription factors. This family of transcription factors has important roles in a wide range of biological functions, including the regulation of cellular growth and differentiation as well as in organ development, vascular development and angiogenesis, and in the regulation of vascular inflammation and remodeling.[14–18]

In vivo and *in vitro* studies have demonstrated that ETS1 is located upstream of an angiogenesis cascade and is crucial for vascular angiogenesis.[19–22] In mice, ETS1 and ETS2 are required for endothelial cell survival and embryonic angiogenesis.[21] In zebrafish, Ets1 has been reported to affect endothelial cell number in axial vessels during vasculogenesis.[22] *In vitro* studies in human umbilical vein endothelial cells (HUVECs) have demonstrated that VEGF amplifies transcription through enhancing ETS1 chromatin occupancy to drive angiogenesis.[19] Despite this, the role of ETS1 in heart development is relatively unknown. In *Ciona intestinalis* and *Drosophila,* ETS1 is a key regulator of cell fate determination and heart cell migration in heart development.[23,24] In *Xenopus*, ETS1 is required in the

cardiac mesoderm and the cardiac neural crest for endocardial development and aortic arch formation, respectively.[25] In chick, reducing ETS1 and ETS2 protein expression results in a coronary and myocardial developmental defect.[26] However, little is known as to the specific roles of ETS1 in the coronary endothelium and endocardium in mammalian heart development, or the mechanisms by which loss of ETS1 results in cardiomyopathy.

In this study, we demonstrate that ETS1 endothelial-specific deletion in mice causes a ventricular non-compaction phenotype, reproducing the phenotype arising from global deletion of ETS1. Our data also reveal that loss of ETS1 significantly represses the levels of Alk1, Cldn5, Sox18, Robo4, Esm1 and Kdr, six direct targets of ETS1 in endothelial cells, resulting in a coronary vascular defect, in association with decreased cardiomyocyte proliferation in the compact zone. Down-regulated ALK1 expression by the loss of ETS1 in the endocardium, along with the up-regulation of TGFβ1 and TGFβ3, was associated with increased TGFBR2/TGFBR1/SMAD2 signaling and increased extracellular matrix (ECM) expression in the trabecular layer, coinciding with increased trabecular cardiomyocyte proliferation.

METHODS

The data, analytical methods, and materials will be available to other researchers for the purposes of reproducing the results or replicating the procedure. Detailed methods and any associated references are provided in the Online Data Supplement. Lists of primers, antibodies and probes used are shown in Online Tables I through III.

Animals

All animal studies were performed in accordance with the National Institutes of Health's Guide for the Care and Use of Laboratory Animals[27] and approved by the Institutional Animal Care and Use Committee of the University of California, San Diego. Global ETS1 null mice were generated as described previously.[28] ETS1 conditional knockout mice were generated by crossing ETS1 flox/flox mice (provided by Michael C. Ostrowski) with Tie2Cre (Jackson Laboratory, #008863) and Pax3Cre (Jackson Laboratory, #005549) mice. Both male and female embryonic mice at different stages from E9.5 to E18.5 were used without genotyping for gender. In addition, 1-year-old male mice were used. The UCSD Animal Care Program maintained all animals and the UCSD Institutional Animal Care and Use Committee approved all experimental procedures. Mice were maintained on a C57/B6 background and genotyping was performed using primers shown in Online Table II.

Statistical Analysis

Statistical analysis was performed using GraphPad Prism 8.4.3. Normal distribution of data was tested by the Kolmogorov-Smirnov normality test as well as the Shapiro-Wilk test and D'Agostino-Pearson normality test. For data distributed normally, values were shown as a mean ± SEM. Unpaired 2-tailed Student's *t* test was used to compare two groups and one-way ANOVA followed by Tukey's multiple comparisons test were used to compare more than two groups. For data not distributed normally or $n<6$, values were shown as medians with interquartile range and a nonparametric test was used to compare two groups.

No experiment-wide/across-test multiple test correction was applied. Multiplicity adjusted P-values were reported where multiple comparisons were made. Otherwise, raw P-values were reported. A value of $P<0.05$ was considered statistically significant. The replicates are biological and so n = number of mice. Power calculations were used for each experiment to ensure the numbers used have a power of more than 80% to detect significant effect sizes ($\alpha=0.05$).

RESULTS

Global deletion of ETS1 results in ventricular non-compaction.

To investigate the role of ETS1 in heart development, we used an ETS1 global knockout (gKO) mouse line in a pure C57/B6 genetic background and analyzed the effects of global loss of ETS1 on heart development. The ETS1 protein was undetectable in gKO embryo (Online Figure IA). As all ETS1 gKO mice died by 1–2 days after birth, embryonic day 18.5 (E18.5) hearts were analyzed first. Global deletion of ETS1 resulted in decreased thickness of the ventricular compact zone and increased thickness of the ventricular trabecular layer at E18.5 (Figure 1A).

To determine the starting point of this abnormal heart phenotype, hematoxylin and eosin histological staining was performed in mice starting from E11.5. No significant differences in compact zone and trabecular layer were observed between gKO and control mice at E11.5 (Online Figure IB). Hearts from E12.5 to E15.5 mice were further analyzed to determine the time course of the development of the abnormal phenotype. In control embryos, the compact zone increased in thickness as embryos progressed from E12.5 to E18.5 (Figure 1A through 1C; Online Figure IC through IE). However, in ETS1 gKO embryos, although the compact zone also grew as embryos progressed from E12.5 to E18.5, the compact zone grew less and was thinner than in the controls at each stage (Figure 1A through 1C; Online Figure IC through IE). Despite the thinner compact zone in the ETS1 gKO mice, the trabecular layer was thicker than in the controls at each stage from E12.5 to E18.5 (Figure 1A and 1B; Online Figure IC through IE). In control embryos, the trabecular layer grew as embryos progressed from E12.5 to E14.5; after E14.5, the thickness of the trabecular layer began to decrease, and the thickness of the trabecular layer was significantly decreased at E18.5 (Figure 1D). However, in ETS1 gKO embryos, the thickness of the trabecular layer was not decreased at E15.5 and E18.5 compared to that at E14.5 (Figure 1D).

The ratios of the thickness of trabecular layer to compact zone from E12.5 to E18.5 showed that although the ratios are reduced as embryos progressed in both control and ETS1 gKO mice, the ratios in gKO mice are significantly higher than in control mice at each stage (Figure 1E). Furthermore, the immunofluorescence of CD31, a marker of all endothelial cells, was used to highlight the endocardium in order to delineate the boundaries of the trabecular layer. The result also showed the decreased thickness of the compact zone and the increased thickness of the trabecular layer in gKO mice relative to those in controls (Figure 1F; Online Figure IF). Thus, these data demonstrate that ETS1 global deletion leads to ventricular non-compaction. In addition to the ventricular non-compaction phenotype, we also found that ETS1 gKO mice have double outlet right ventricle (DORV). Global deletion

of ETS1 didn't impact atrioventricular (AV) valvular development (Online Figure IG) or endothelial to mesenchymal transition (EMT) of the AV cushions (Online Figure IH and I I).

Global deletion of ETS1 results in a coronary vascular defect.

The ETS1 gKO mouse ventricle not only showed a thinner compact zone but also contained fewer endothelial cells in the compact zone, suggesting a coronary vascular defect (Figure 2A and 2B). Whole heart CD31 immunofluorescence images at E13.5 and E14.5 also demonstrated fewer endothelial cells in the compact zone in the ETS1 gKO mouse ventricles (Figure 2C), consistent with a coronary vascular angiogenesis defect. To confirm that global deletion of ETS1 resulted in a coronary vascular defect, whole-mount immunofluorescence was performed to visualize the coronary vasculature. As the first coronary capillary plexus forms on the surface of the heart from the sinus venosus (SV) and spreads to the entire surface of the heart at ~E11.5-E12.5 in the mouse embryo,[29] whole-mount immunofluorescence was first performed at E12.5 on the hearts in gKO mice and littermate controls. At E12.5, although the coronary vasculature has spread on the dorsal side of the heart in both the gKO mice and the controls, the coronary vascular growth was stunted and the area covered by coronary vasculature was decreased in gKO mice, indicating a defect in angiogenesis (Figure 2D and 2F). At E14.5, the coronary vessels emerge from the midline of the ventral side of the heart and migrate laterally to populate the ventral side together with the coronary vessels spreading from the dorsal side. The whole-mount immunofluorescence performed at E14.5 showed that the coronary vascular growth was stunted and the area covered by coronary vasculature was significantly decreased in gKO mice, also indicating an angiogenesis defect (Figure 2E and 2F). We next analyzed the coronary vascular structure at E18.5. The E18.5 gKO embryos also exhibited dramatic defects with truncated coronary vessels and decreased arborization (Figure 2G).

Together, these data demonstrate that global deletion of ETS1 causes a coronary vasculature developmental defect. It has been reported that defects in coronary angiogenesis leads to ventricular non-compaction in mice.[6] The coronary vasculature is required to ensure proper myocardial nourishment and development of the compact zone.[6,8,9] Our study provides further evidence suggesting that the coronary vascular defect contributes to ventricular non-compaction in ETS1 gKO mice.

ETS1 endothelial deletion recapitulates the ETS1 global knockout ventricular non-compaction phenotype.

To further investigate the role of ETS1 in heart development, a conditional knockout mouse line was used to generate a deletion of ETS1 in two different cardiac cellular lineages: the endothelium (including the endocardium and the coronary vascular endothelium) and the neural crest, in which ETS1 is expressed.[11] A Tie2Cre driver line was used to delete ETS1 in endothelial cells and endocardial cells. ETS1 immunofluorescence showed undetectable ETS1 protein in endocardium and SV endothelium in endothelial conditional knockout (eKO) embryos at E11.5, which are also the two sources of the coronary endothelium (Figure 3A). Deletion of ETS1 in endothelial cells resulted in decreased thickness of the compact zone and increased thickness of the trabecular layer from E12.5 to E18.5 (Figure 3B and 3C; Online Figure IIA through IIC), recapitulating the global knockout phenotype.

This phenotype was associated with decreased survival in eKO embryos, and the hearts of the dead eKO embryos displayed severe thinning of the compact zone (Online Figure III). In contrast, conditional deletion of ETS1 in neural crest cells (NCCs) did not affect the growth of the compact zone and the trabecular layer (Figure 3D).

We next measured the thickness of the compact zone and the trabecular layer of left ventricle in control and endothelial eKO mice from E12.5 to E18.5 to determine the time course of the development of the ventricular non-compaction phenotype. In control embryos, the compact zone grew dramatically as embryos progressed from E12.5 to E18.5 and the thickness of the compact zone increased significantly (Figure 3E). However, in eKO embryos, as in gKO embryos, although the compact zone also grew as embryos progressed from E12.5 to E18.5, the compact zone was thinner than that in the controls at each stage (Figure 3E). Also as in gKO mice, despite the thinner compact zone in the ETS1 eKO mice, the trabecular layer was thicker than that in the controls at each stage from E12.5 to E18.5 (Figure 3F). In control embryos, the trabecular layer grew as embryos progressed from E12.5 to E14.5; after E14.5, the thickness of the trabecular layer began to decrease, and the thickness of the trabecular layer was significantly decreased at E18.5 (Figure 3F). However, in eKO embryos, the thickness of the trabecular layer was not decreased at E15.5 and E18.5 compared to that at E14.5 (Figure 3F).

Calculating the ratios of the thickness of trabecular layer to compact zone in left ventricle showed that although the ratios were reduced as embryos progressed from E12.5 to E18.5 in both control and eKO mice, the ratios in eKO mice were significantly higher than in the control mice at each stage (Figure 3G). Furthermore, CD31 immunofluorescence also showed the decreased thickness of the compact zone and increased thickness of the trabecular layer in eKO mice (Figure 3H; Online Figure IID). In addition, as it is reported that ventricular non-compaction is associated with increased cardiomyocyte maturation[30], qPCR was performed on samples from E15.5 control and eKO embryonic mouse ventricles to determine the expression levels of cardiomyocyte maturation markers. Tnnt2, Tnni1, Tnni3 and Myh6 were up-regulated in ETS1 eKO mice compared to littermate controls (Online Figure IIE). Taken together, the ventricular non-compaction phenotype in the endothelial conditional deletion faithfully replicates that of the global knockout mouse embryos. In addition, we investigated the effects of ETS1 endothelial deletion in adult mice. On gross examination of one year-old eKO mouse hearts, we found their coronary arteries had decreased branching compared to control mice (Online Figure IIF). We also found that one year-old eKO mice had a thinned right ventricular wall, along with a slightly thicker left ventricular wall (Online Figure IIG and IIH). Notably, the one mouse that died at age one year had a severely dilated right ventricle, in contrast to control and the three surviving one year-old mice analyzed (Online Figure IIG).

Next, we assessed cardiomyocyte proliferation by measuring the percentage of phospho-Histone H3 (PH3) positive cardiomyocytes, which revealed decreased cardiomyocyte proliferation in the compact zone and increased proliferation in the trabecular layer at E12.5 and E13.5 in eKO mice (Figure 3I and 3J). In addition, we did not find any differences in cardiomyocyte apoptosis between E13.5 control and eKO mice by TUNEL assay (Online Figure II I and IIJ). Together, these data demonstrate that loss of ETS1 in endothelial

cells leads to ventricular non-compaction through a differential effect on cardiomyocyte proliferation in the compact zone and trabecular layer.

ETS1 endothelial deletion results in a coronary vascular defect.

The coronary vasculature is critical for the development of the compact zone of the ventricular myocardium during embryogenesis, specifically including a requirement for coronary endothelial cells for cardiomyocyte proliferation.[6,8,9,31] We have demonstrated that global deletion of ETS1 causes a coronary vasculature developmental defect. Therefore, we investigated whether there is a coronary vascular defect in the endothelial conditional deletion that may underlie the decreased cardiomyocyte proliferation in the compact zone. As in gKO mice, there were markedly fewer endothelial cells in the compact zone in E13.5 and E14.5 ETS1 eKO mice, indicating a coronary vascular defect (Figure 4A and 4B). Whole heart CD31 immunofluorescence images at E13.5 and E14.5 also demonstrated fewer endothelial cells in the compact zone in the ETS1 eKO mouse ventricles (Figure 4C), consistent with a coronary vascular angiogenesis defect. To confirm that endothelial deletion of ETS1 resulted in the coronary vascular defect, we performed whole-mount immunofluorescence to characterize the coronary vasculature at E12.5. The coronary vascular growth was stunted on the dorsal side of the heart and the area covered by coronary vasculature was significantly decreased in eKO mice, indicating a defect in angiogenesis (Figure 4D and 4F). Whole-mount immunofluorescence performed at E14.5 revealed the stunted coronary vascular growth and the decreased area covered by the coronary vasculature on the ventral side of the heart in eKO mice, also indicating an angiogenesis defect (Figure 4E and 4F). E18.5 eKO embryos also exhibited dramatic defects with truncated coronary vessels and decreased arborization (Figure 4G). In contrast, conditional deletion of ETS1 in NCCs did not affect the coronary vascular development (Online Figure IVA and IVB).

To further investigate the role of ETS1 on coronary endothelial cells, ETS1 siRNA was used to silence the ETS1 gene in cultured human coronary artery endothelial cells (HCAECs). After treatment for 48 hours, ETS1 siRNA suppressed ETS1 mRNA expression (Figure 5R) and there was a concomitant decrease in HCAEC tube formation (Figure 5S and 5T) and migration (Online Figure IVC and IVD), *in vitro*. Taken together, these data indicate that endothelial deletion of ETS1 causes a coronary vasculature developmental defect in association with decreased cardiomyocyte proliferation and a hypoplastic compact zone, reproducing the gKO phenotype.

Loss of ETS1 in endothelial cells represses Alk1, Cldn5, Sox18, Robo4, Esm1 and Kdr, impairing coronary vascular development.

To begin to define the gene regulatory network involving ETS1 in ventricular development, RNA sequencing (RNA-Seq) was performed on samples from E12.5 control and gKO mouse ventricles, a time point when the non-compaction phenotype became apparent. Comparing the differential gene expression between control and gKO mice revealed that 168 genes were significantly down-regulated and 386 were significantly up-regulated in gKO mice. Gene ontology (GO) enrichment analysis identified the top biological processes as endothelium development, angiogenesis, circulatory system development and extracellular

structure organization (Figure 5A), consistent with our findings of a coronary vascular endothelial and endocardial defect. Hypoxia-related genes were also investigated. RNA-Seq results from E12.5 control and ETS1 gKO ventricles revealed nine potential up-regulated hypoxia-related genes (Online Figure IVE). To determine whether these hypoxia-related genes are increased in eKO mice, qPCR was performed on samples from E13.5 embryonic mouse ventricles. The qPCR results confirmed that Bnip3, Egln3, Vegfa, Egr1, Meg3, Egln1 and Higd1a were up-regulated in ETS1 eKO mice compared to littermate controls (Online Figure IVF).

To define how loss of ETS1 in endothelial cells leads to a coronary vascular defect, we focused on the down-regulated genes that are involved in angiogenesis, identified by the GO enrichment analysis, including Alk1, Pik3r6, Thy1, Cldn5, Sox18, Robo4, Ceacam1, Esm1, Gpr4, Notch4, Flt4, Kdr, Pf4 and Ppp1r16b (Figure 5B and Online Figure IVG). In order to explore which genes are direct targets of ETS1, we analyzed the published ETS1 chromatin immunoprecipitation sequencing (ChIP-seq) dataset from HUVECs.[19] Combined analysis of the ETS1 ChIP-seq dataset with available RNAPII, H3K4me3 and H3K27ac ChIP-seq data revealed that ETS1 ChIP peaks were present in promoters or enhancers of Alk1, Cldn5, Sox18, Robo4, Esm1, Notch4, Kdr and Ppp1r16b (Online Figure V). Quantitative polymerase chain reaction (qPCR) on samples from E12.5 mouse ventricles confirmed that Alk1, Cldn5, Sox18, Robo4, Esm1 and Kdr, six important angiogenesis-relevant genes in endothelial cells, were significantly down-regulated in ETS1 eKO mice compared to littermate controls (Figure 5C).

To confirm Alk1, Cldn5, Sox18, Robo4, Esm1 and Kdr are direct targets for ETS1 in mice, ChIP-qPCR was performed on E12.5 mouse heart ventricles. JASPAR was used to predict potential ETS1 transcription factor binding sites. For each gene, several potential binding sites in the promoter region were revealed and two potential binding sites with the highest score were selected for the further ChIP-qPCR (Figure 5D). The ChIP-qPCR results revealed significant enrichment of ETS1 binding sites in the promoter regions of Alk1, Cldn5, Sox18, Robo4, Esm1 and Kdr (Figure 5E), demonstrating they are direct targets of ETS1 in mice. To further investigate the expression levels of these six genes in coronary endothelial cells, RNAscope *in situ* hybridization (ISH) was performed at E13.5. Alk1, Cldn5, Sox18, Robo4, Esm1 and Kdr mRNA levels were decreased in coronary endothelial cells in ETS1 eKO mice compared to littermate controls (Figure 5F through 5Q).

To further investigate the role of the six angiogenesis-related genes on coronary endothelial cells, siRNA of each gene or a cocktail of all six siRNAs (6A siRNA) are used to silence these six genes individually or together in HCAECs. After treatment for 48 hours, Alk1, Cldn5, Sox18, Robo4, Esm1 and Kdr siRNA suppressed their mRNA expression respectively (Figure 5R). Although Alk1 siRNA treatment increased HCAEC tube formation, siRNA treatment of each of the other five genes decreased HCAEC tube formation (Figure 5S and 5T). Silencing these six angiogenesis-related genes together also decreased HCAEC tube formation (Figure 5S and 5T). Taken together, these results demonstrate that loss of ETS1 in endothelial cells causes coronary vascular defects and down-regulates genes involved in angiogenesis.

Endothelial-specific deletion of ETS1 increases the expression of extracellular matrix genes in the trabecular layer.

Based on the RNA-seq results from E12.5 control and ETS1 gKO ventricles, GO enrichment analysis also revealed many up-regulated genes that contribute to extracellular structure organization (Figure 5A), including numerous extracellular matrix (ECM) genes (Fn1, Lama1, Col1a1, Fbn1 and Acan) as well as integrin genes (Itgb4, Itga6, Itga7, Itga8, Itga9, Itgal, Itgam and Itgav) (Figure 6A and Online Figure IVG), which function as receptors for ECMs required for initiating intracellular signaling cascades.[32,33] It has been reported that ECMs are critical for cardiomyocyte proliferation.[32,33] Increased ECM synthesis has been reported to be involved in the pathogenesis of non-compaction cardiomyopathy.[34] Specifically, persistent ECM synthesis enables enhanced trabecular growth in the trabecular layer.[34]

To determine whether the increased cardiomyocyte proliferation in the trabecular layer in eKO mice might be due to the increased expression of ECM genes, qPCR was performed on samples from E12.5 embryonic mouse ventricles. The qPCR results confirmed that Fn1, Lama1, Col1a1, Fbn1 and Acan, five ECM genes identified by the GO enrichment analysis, were up-regulated in ETS1 eKO mice compared to littermate controls (Figure 6B). In addition, the qPCR analysis also showed that Postn, another ECM gene, was up-regulated in ETS1 eKO mice compared to littermate controls (Figure 6B). To further investigate the expression patterns and levels of these ECM genes, immunofluorescence and RNAscope ISH were performed. Increased protein levels of Fibronectin, Periostin, Laminin and Collagen1 were deposited between the endocardium and trabecular myocardium in ETS1 eKO mice compared to littermate controls at E12.5 and E13.5 (Figure 6C through 6J; Online Figure VIA through VIH). Fbn1 and Acan mRNA levels were also increased in the trabecular layer in ETS1 eKO mice at E12.5 and E13.5 (Figure 6K and 6N; Online Figure VI I and VIL). In contrast, these genes were expressed in compact zone cardiomyocytes at low levels (Figure 6C, 6E, 6G, 6I, 6K and 6M), consistent with a specific effect of ECM components on trabecular growth. Together, these data indicate that endothelial-specific deletion of ETS1 increases the expression of ECM genes in the trabecular layer, in association with increased trabecular cardiomyocyte proliferation and growth.

Deficiency of ETS1 increases ECM expression through intensifying TGFBR2 /TGFBR1/ SMAD2 signaling pathway.

Loss of ETS1 in endothelial cells significantly down-regulated the levels of Alk1, Cldn5, Sox18, Robo4, Esm1 and Kdr (Figure 5C). Among these genes, Alk1, which encodes a type I cell-surface receptor for the TGFβ superfamily of ligands, was most significantly changed, with a four-fold decrease (Figure 5C). To further investigate the expression level and pattern of Alk1, RNAscope ISH was performed. Though Alk1 is predominantly expressed in endocardial cells, coronary endothelial cells and epicardial cells, the mRNA levels of ALK1 were only decreased in endocardium and in coronary endothelium in eKO mice compared controls (Figure 7A and 7B; Online Figure VIIA and VIIB; Figure 5F and 5G). Next, we investigated the phosphorylation level of Smad1/5, the downstream effector of ALK1. The results of immunofluorescence demonstrated that the number of phosphorylated Smad1/5 positive cells was decreased in endocardium as well as in coronary endothelium, paralleling

the decreased ALK1 expression in the absence of ETS1 (Figure 7C and 7D; Online Figure VIIC and VIID). To further confirm the effect of ETS1 on ALK1, western blot analyses were performed on lysates from E12.5 and E13.5 ventricles. The protein levels of ALK1 were eight-fold and three-fold reduced at E12.5 and E13.5 respectively in eKO mice, and the phosphorylated protein levels of Smad1/5 were three-fold and two-fold reduced at E12.5 and E13.5 respectively in eKO mice, relative to those in controls (Figure 7E and 7F; Online Figure VIIE and VIIF). To further investigate the expression level of total-Smad5, western blot analyses were performed on lysates from E12.5 and E13.5 ventricles and RNAscope ISH was performed at E13.5. The expression levels of Smad5 were not altered in eKO mice compared to littermate controls (Online Figure VIIIA through VIIIC).

TGFβ dynamically regulates angiogenesis and ECM expression in endothelial cells. TGFβ first binds to TGFBR2 and then recruits TGFBR1.[35] TGFβ signaling through TGFBR1/Smad2/3 induces ECM expression.[36,37] This TGFβ/TGFBR2/TGFBR1 complex also can recruit ALK1, an antagonistic mediator of the TGFBR1/Smad2/3 pathway, positively regulating angiogenesis and negatively regulating ECM expression.[35,37] Therefore, Western blot analyses were performed on lysates from E12.5 and E13.5 ventricles to investigate the levels of TGFBR2 and TGFBR1. The expression levels of TGFBR2 and TGFBR1 were significantly increased in eKO mice relative to those in controls (Figure 7G and 7H; Online Figure IXA and IXB). To further investigate the expression levels and patterns of TGFBR2 and TGFBR1, immunofluorescence was performed. The expression of TGFBR2 was up-regulated both in the endocardium and in the trabecular cardiomyocytes in eKO mice compared to that in controls. In contrast, no obvious differences were found in the expression of TGFBR2 in the compact zone between eKO mice and controls (Figure 7I and 7J; Online Figure IXC and IXD). The level of TGFBR1 was also up-regulated in endocardium and in cardiomyocytes in the trabecular layer in eKO mice compared to that in controls, but not in the compact zone (Figure 7K and 7L; Online Figure IXE and IXF). We further investigated the phosphorylated protein level of Smad2, the downstream effector of TGFBR1. Western blot analyses using lysates from E12.5 and E13.5 ventricles revealed that the phosphorylated protein levels of Smad2 were significantly increased in eKO ventricles relative to that in controls (Figure 7G and 7H; Online Figure IXA and IXB). The results of immunofluorescence demonstrated that the phosphorylated levels of Smad2 were up-regulated in endocardium and trabecular cardiomyocytes in eKO mice compared to that in controls, but not in the compact zone, as for TGFBR2 and TGFBR1 (Figure 7M and 7N; Online Figure IXG and IXH). To further investigate the expression level of total-Smad2, western blot analyses were performed on lysates from E12.5 and E13.5 ventricles and RNAscope ISH was performed at E13.5. The expression levels of Smad2 were not altered in eKO mice compared to littermate controls (Online Figure VIIIA, VIIIB and VIIID).

Next, we performed Western blot analyses using lysates from E12.5 and E13.5 ventricles to explore the expression levels of the three TGFβ ligands. The levels of TGFβ1 and TGFβ3 were significantly up-regulated in eKO mice compared to those in controls, but the level of TGFβ2 was not altered (Figure 7O and 7P; Online Figure IX I and IXJ). These data indicate that the repression of ALK1 in the endocardium due to the deletion of ETS1, combining with the up-regulation of TGFβ1 and TGFβ3, leads to increased

TGFBR2/TGFBR1/SMAD2 signaling and increased ECM expression in endocardial cells and cardiomyocytes in the trabecular layer.

DISCUSSION

Although controversial,[38] human genome-wide association studies have demonstrated that non-compaction cardiomyopathy is a genetic form of cardiomyopathy caused by mutations in genes encoding sarcomeric, cytoskeletal and nuclear membrane proteins.[8,39,40] Recent studies have revealed that dysfunction of the coronary endothelium and endocardium are also associated with non-compaction cardiomyopathy.[6–9] *In vivo* and *in vitro* studies have demonstrated that ETS1 is essential for vascular angiogenesis.[19–22] However, the role of ETS1 in heart development is relatively unknown. In this study, we investigate the specific roles of ETS1 in the coronary endothelium and endocardium in murine heart development and the mechanisms by which loss of ETS1 results in a coronary vascular and non-compaction ventricular phenotype (Figure 8). Our findings reveal that endothelial-specific deletion of ETS1 recapitulated the ventricular non-compaction phenotype observed in ETS1 gKO mice, along with the impaired coronary vascular development and the increased trabecular ECM expression, indicating that ventricular non-compaction is a direct consequence of ETS1 deficiency in the coronary endothelium and endocardium. There was significant phenotypic variation in the ETS1 eKO mice. Specifically, we observed a small subset of embryos that died prenatally and were found to have a severely thinned, nearly absent compact zone. The majority of ETS1 eKO mice survived to adulthood. We found that one year-old ETS1 eKO mice had a thinned right ventricular wall, and that the left ventricular wall was slightly thickened compared to age-matched controls. Of note, the one year-old mouse that died had a markedly dilated right ventricle. The basis for this phenotypic variability is unknown and will be the focus of future studies.

Previous studies have demonstrated that decreased compact zone cardiomyocyte proliferation and increased trabecular cardiomyocyte proliferation underlie ventricular non-compaction.[6,41,42] In this study, we demonstrate that loss of ETS1 causes decreased cardiomyocyte proliferation in the compact zone and a concomitant increase in cardiomyocyte proliferation in the trabecular layer during early stages of ventricular development. Our studies are consistent with previous studies demonstrating that coronary vascular endothelial cells are required for compact myocardial growth; while ECMs are essential for trabecular cardiomyocyte proliferation.[6,43,44] Our results indicate that the ETS1 transcription factor simultaneously regulates both of these processes and provide a molecular basis for the differential effect on cardiomyocyte proliferation in these two subpopulations of ventricular cardiomyocytes. Furthermore, since ETS1 is not expressed in cardiomyocytes during murine heart development,[11] these results provide a molecular basis for the non cell-autonomous effect on cardiomyocyte proliferation and growth in the developing ventricles.

Our study defines a gene regulatory network involving ETS1 in the coronary vascular endothelium and endocardium. GO enrichment analysis of RNA-Seq performed on ventricular tissue from E12.5 control and ETS1 gKO mouse embryos revealed a set of down-regulated genes that are involved in endothelium development and angiogenesis and a set of up-regulated genes functioning in ECM organization. Specifically, the gene expression

analyses demonstrate that endothelial deletion of ETS1 increases expression of six ECM genes in the trabecular layer, including Fn1, Postn, Lama1, Col1a1, Fbn1 and Acan. We also demonstrate that endothelial-specific deletion of ETS1 represses the levels of Alk1, Cldn5, Sox18, Robo4, Esm1 and Kdr, six important angiogenesis-relevant genes in endothelial cells, which are demonstrated to be direct targets of ETS1. Silencing these six angiogenesis-related genes together *in vitro* decreased HCAEC tube formation. Thus, down-regulated expression of these genes together by loss of ETS1 in the coronary endothelium represses the coronary vascular angiogenesis in ETS1 eKO mice. We also found that down-regulation of ALK1 expression in endocardium due to the loss of ETS1, along with up-regulation of TGFβ1 and TGFβ3, occurred with increased TGFBR2/TGFBR1/SMAD2 signaling and increased ECM gene expression in the trabecular layer. Taken together, we demonstrate that endothelial and/or endocardial ETS1 is essential for regulating ventricular cardiomyocyte proliferation and homoeostasis as well as for coronary vascular growth during heart development. Besides the ventricular non-compaction phenotype, which we found to be most severe in a small subset of embryos that die prenatally, we also found the ETS1 gKO mice have DORV, which is the most common cause of the postnatal death in C57/B6 mice. Specifically, these mice die shortly after birth due to pulmonary over-circulation resulting from a large intracardiac left to right shunt. We have found that DORV is due to a cell-autonomous neural crest cell migration defect caused by deletion of ETS1 in NCCs.

JBS is a rare chromosomal disorder characterized by deletions in distal 11q, resulting in multiple developmental defects including CHDs.[2] Half of human patients with JBS have hemodynamically significant congenital heart defects, frequently requiring lifesaving medical therapies and/or surgical interventions. The molecular basis for the incomplete penetrance and variation in the specific cardiac phenotype in these patients is unknown. We have found varying levels of ETS1 mRNA expressed from the intact allele in neural crest cells derived from JBS patient-specific induced pluripotent stem cells. Specifically, in one patient with HLHS and a neural crest cell migration defect, expression from the “normal” allele was virtually absent, i.e. mimicking a mouse null genotype. In a second patient with complex congenital heart disease and a neural crest cell migration defect, there was a normal level of ETS1 mRNA, suggesting decreased function of ETS1 expressed from the intact allele. Together, these results may explain, at least in part, the molecular basis for incomplete penetrance for congenital heart disease that occurs in JBS. Interestingly, we also found that mutations in several of the ETS1 direct downstream target genes that we have identified in the current study have been reported to be associated with some of the same congenital heart defects that occur in JBS, including in ALK1 (total anomalous pulmonary venous connections and pulmonary arterial hypertension) and ROBO4 (bicuspid aortic valve). We speculate that at least one basis for the different specific congenital heart defects occurring between individuals may be due to relative differences in sensitivity to ETS1 gene dosage between the downstream target genes, possibly due to genetic polymorphisms.

Loss of ETS1 is the cause of CHDs in JBS,[11] and ventricular non-compaction can occur in JBS. Another CHD that commonly occurs in JBS is HLHS. Interestingly, ventricular non-compaction and HLHS have been reported to occur in the same patient,[45,46] suggesting that these two CHDs may be mechanistically related. In ETS1 eKO mice, we have also observed, rarely, a diminutive ventricular chamber volume (one of the hallmarks of HLHS)

due to severe expansion of the trabecular layer. This suggests the intriguing possibility that at least some anatomic subsets of HLHS could be due to a more extreme effect on trabecular cardiomyocyte proliferation during heart development, leading to a hypoplastic ventricular chamber volume. Other CHDs that occur in JBS include septal and outflow tract defects, which are likely to be due impaired neural crest cell function.[11,25] These observations suggest that the multiple functions of ETS1 affecting both vascular endothelial/endocardial and neural crest lineages likely determine the specific cardiac phenotype in patients with JBS and is dependent on the genetic background, e.g. genetic polymorphisms in genes regulated by ETS1, an exciting area for future investigation. Our study also provides a molecular basis by which coronary artery anomalies can be associated with other structural heart defects. Defects in the coronary vasculature can have important clinical implications, including why some patients with complex CHDs develop early heart failure.

Understanding the molecular and cellular mechanisms of ETS1 in the coronary vascular endothelium and endocardium in normal heart development will enhance our understanding of the coronary vascular system and endocardium in the pathogenesis of many congenital heart defects. Our study demonstrates a critical role for ETS1 in ventricular and coronary vascular development. Consequently, further delineation of the gene regulatory network(s) involving ETS1 in heart development will enhance our understanding of the molecular mechanisms underlying many of the most common and severe congenital heart defects, and will lead to improved approaches for the treatment of patients with congenital heart disease.

Supplementary Material

Refer to Web version on PubMed Central for supplementary material.

ACKNOWLEDGEMENTS

The authors would like to thank Dr. Michael Ostrowski for providing the ETS1 floxed allele mice. The authors also would like to thank UCSD School of Medicine Microscopy Core (Grant: NINDS P30 NS047101) for the invaluable technical support.

SOURCES OF FUNDING

Funding for this research was provided by the cast and crew of “How I Met Your Mother”, The Hertz Family Foundation, The Rady Children’s Hospital Foundation, The 11q Research and Resource Group, The Chloe Duyck Memorial Fund, and The Warren J. and Betty C. Zable Foundation.

Non-standard Abbreviations and Acronyms

AV	atrioventricular
CHD	congenital heart defect
DORV	double outlet right ventricle
ECM	extracellular matrix
EMT	endothelial to mesenchymal transition
eKO	endothelial conditional knockout

ETS	E26 Transformation Specific
gKO	global knockout
GO	gene ontology
HLHS	hypoplastic left heart syndrome
HCAEC	human coronary artery endothelial cell
HUVEC	human umbilical vein endothelial cell
ISH	RNAscope *in situ* hybridization
JBS	Jacobsen syndrome
SV	sinus venosus

REFERENCES

1. Bruneau BG, Srivastava D. Congenital heart disease: entering a new era of human genetics. Circ Res. 2014;114:598–599. [PubMed: 24526674]
2. Grossfeld PD, Mattina T, Lai Z, Favier R, Jones KL, Cotter F, Jones C. The 11q terminal deletion disorder: a prospective study of 110 cases. Am J Med Genet. 2004;129A:51–61. [PubMed: 15266616]
3. Mattina T, Perrotta CS, Grossfeld P. Jacobsen syndrome. Orphanet J Rare Dis. 2009;4:9. [PubMed: 19267933]
4. Grego-Bessa J, Luna-Zurita L, del Monte G, Bolós V, Melgar P, Arandilla A, Garratt AN, Zang H, Mukouyama YS, Chen H, Shou W, Ballestar E, Esteller M, Rojas A, Pérez-Pomares JM, de la Pompa JL. Notch signaling is essential for ventricular chamber development. Dev Cell. 2007;12:415–429. [PubMed: 17336907]
5. Han P, Bloomekatz J, Ren J, Zhang R, Grinstein JD, Zhao L, Burns CG, Burns CE, Anderson RM, Chi NC. Coordinating cardiomyocyte interactions to direct ventricular chamber morphogenesis. Nature. 2016;534:700–704. [PubMed: 27357797]
6. Rhee S, Chung JI, King DA, D'amato G, Paik DT, Duan A, Chang A, Nagelberg D, Sharma B, Jeong Y, Diehn M, Wu JC, Morrison AJ, Red-Horse K. Endothelial deletion of Ino80 disrupts coronary angiogenesis and causes congenital heart disease. Nat Commun. 2018;9:368. [PubMed: 29371594]
7. Chen H, Zhang W, Sun X, Yoshimoto M, Chen Z, Zhu W, Liu J, Shen Y, Yong W, Li D, Zhang J, Lin Y, Li B, VanDusen NJ, Snider P, Schwartz RJ, Conway SJ, Field LJ, Yoder MC, Firulli AB, Carlesso N, Towbin JA, Shou W. Fkbp1a controls ventricular myocardium trabeculation and compaction by regulating endocardial Notch1 activity. Development. 2013;140:1946–1957. [PubMed: 23571217]
8. D'Amato G, Luxán G, del Monte-Nieto G, Martínez-Poveda B, Torroja C, Walter W, Bochter MS, Benedito R, Cole S, Martinez F, Hadjantonakis A, Uemura A, Jiménez-Borreguero LJ, de la Pompa JL. Sequential Notch activation regulates ventricular chamber development. Nat Cell Biol. 2016;18:7–20. [PubMed: 26641715]
9. D'Amato G, Luxán G, de la Pompa JL. Notch signalling in ventricular chamber development and cardiomyopathy. FEBS J. 2016;283:4223–4237. [PubMed: 27260948]
10. Grossfeld P, Nie S, Lin L, Wang L, Anderson RH. Hypoplastic Left Heart Syndrome: A New Paradigm for an Old Disease? J Cardiovasc Dev Dis.2019;6(1).
11. Ye M, Coldren C, Benson W, Goldmuntz E, Ostrowski M, Watson D, Perryman B, Grossfeld P. Deletion of ETS-1, a gene in the Jacobsen syndrome critical region, causes ventricular septal defects and abnormal ventricular morphology in mice. Hum Mol Genet. 2010;19:648–656. [PubMed: 19942620]

12. Ye M, Xu L, Fu M, Chen D, Mattina T, Zufardi O, Rossi E, Bush KT, Nigam SK, Grossfeld P. Gene-targeted deletion in mice of the Ets-1 transcription factor, a candidate gene in the Jacobsen syndrome kidney “critical region,” causes abnormal kidney development. Am J Med Genet A. 2019;179:71–77. [PubMed: 30422383]
13. Tootleman E, Malamut B, Akshoomoff N, Mattson SN, Hoffman HM, Jones MC, Printz B, Shiryaev SA, Grossfeld P. Partial Jacobsen syndrome phenotype in a patient with a de novo frameshift mutation in the ETS1 transcription factor. Cold Spring Harb Mol Case Stud. 2019;5.
14. Liu F, Patient R. Genome-wide analysis of the zebrafish ETS family identifies three genes required for hemangioblast differentiation or angiogenesis. Circ Res. 2008;103:1147–1154. [PubMed: 18832752]
15. Craig MP, Sumanas, S. ETS transcription factors in embryonic vascular development. Angiogenesis. 2016;19:275–285. [PubMed: 27126901]
16. Sato Y Role of ETS family transcription factors in vascular development and angiogenesis. Cell Struct Funct. 2001;26:19–24. [PubMed: 11345500]
17. Pham VN, Lawson ND, Mugford JW, Dye L, Castranova D, Lo B, Weinstein BM. Combinatorial function of ETS transcription factors in the developing vasculature. Dev Biol. 2007;303:772–783. [PubMed: 17125762]
18. Craig MP, Grajevskaja V, Liao HK, Balciuniene J, Ekker SC, Park JS, Essner JJ, Balciunas D, Sumanas S. Etv2 and fli1b function together as key regulators of vasculogenesis and angiogenesis. Arterioscler Thromb Vasc Biol. 2015;35:865–876. [PubMed: 25722433]
19. Chen J, Fu Y, Day DS, Sun Y, Wang S, Liang X, Gu F, Zhang F, Stevens SM, Zhou P, Li K, Zhang Y, Lin RZ, Smith LEH, Zhang J, Sun K, Melero-Martin JM, Han Z, Park PJ, Zhang B, Pu WT. VEGF amplifies transcription through ETS1 acetylation to enable angiogenesis. Nat Commun. 2017;8:383. [PubMed: 28851877]
20. Hashiya N, Jo N, Aoki M, Matsumoto K, Nakamura T, Sato Y, Ogata N, Ogihara T, Kaneda Y, Morishita R. In vivo evidence of angiogenesis induced by transcription factor Ets-1: Ets-1 is located upstream of angiogenesis cascade. Circulation. 2004;109:3035–3041. [PubMed: 15173033]
21. Wei G, Srinivasan R, Cantemir-Stone CZ, Sharma SM, Santhanam R, Weinstein M, Muthusamy N, Man AK, Oshima RG, Leone G, Ostrowski MC. Ets1 and Ets2 are required for endothelial cell survival during embryonic angiogenesis. Blood. 2009;114:1123–1130. [PubMed: 19411629]
22. Chetty SC, Sumanas S. Ets1 functions partially redundantly with Etv2 to promote embryonic vasculogenesis and angiogenesis in zebrafish. Dev Biol. 2020;465:11–22. [PubMed: 32628937]
23. Davidson B, Shi W, Beh J, Christiaen L, Levine M. FGF signaling delineates the cardiac progenitor field in the simple chordate, Ciona intestinalis. Genes Dev. 2006;20:2728–2738. [PubMed: 17015434]
24. Alvarez AD, Shi W, Wilson BA and Skeath JB. pannier and pointedP2 act sequentially to regulate Drosophila heart development. Development. 2003;130:3015–3026. [PubMed: 12756183]
25. Nie S, Bronner M. Dual developmental role of transcriptional regulator Ets1 in Xenopus cardiac neural crest vs. heart mesoderm. Cardiovasc Res. 2015;106:67–75. [PubMed: 25691536]
26. Lie-Venema H, Gittenberger-de Groot AC, van Empel LJ, Boot MJ, Kerkdijk H, de Kant E, DeRuiter MC. Ets-1 and Ets-2 transcription factors are essential for normal coronary and myocardial development in chicken embryos. Circ Res. 2003;92:749–756. [PubMed: 12637368]
27. National Research Council. Guide for the Care and Use of Laboratory Animals (National Academies Press, Washington, DC), 8th Ed. 2011.
28. Barton K, Muthusamy N, Fischer C, Ting CN, Walunas TL, Lanier LL, Leiden JM. The Ets-1 transcription factor is required for the development of natural killer cells in mice. Immunity. 1998;9:555–563. [PubMed: 9806641]
29. Nakano A, Nakano H, Smith KA, Palpant NJ. The developmental origins and lineage contributions of endocardial endothelium. Biochim Biophys Acta. 2016;1863:1937–1947. [PubMed: 26828773]
30. Rhee S, Paik DT, Yang JY, Nagelberg D, Williams I, Tian L, Roth R, Chandy M, Ban J, Belbachir N, Kim S, Zhang H, Phansalkar R, Wong KM, King DA, Valdez C, Winn VD, Morrison AJ, Wu JC, Red-Horse K. Endocardial/endothelial angiocrines regulate cardiomyocyte development and

maturation and induce features of ventricular non-compaction. Eur Heart J. 2021;42:4264–4276. [PubMed: 34279605]

31. Luxán G, D'Amato G, MacGrogan D, de la Pompa JL. Endocardial Notch Signaling in Cardiac Development and Disease. Circ Res. 2016;118:e1–e18. [PubMed: 26635389]
32. Miao Y, Tian L, Martin M, Paige SL, Galdos FX, Li JB, Klein A, Zhang H, Ma N, Wei Y, Stewart M, Lee S, Moonen J, Zhang B, Grossfeld P, Mital S, Chitayat D, Wu JC, Rabinovitch M, Nelson TJ, Nie S, Wu SM, Gu M. Intrinsic Endocardial Defects Contribute to Hypoplastic Left Heart Syndrome. Cell Stem Cell. 2020;27:574–589. [PubMed: 32810435]
33. Hornberger LK, Singhroy S, Cavalle-Garrido T, Tsang W, Keeley F, Rabinovitch M. Synthesis of extracellular matrix and adhesion through beta(1) integrins are critical for fetal ventricular myocyte proliferation. Circ Res. 2000;87:508–515. [PubMed: 10988244]
34. del Monte-Nieto G, Ramialison M, Adam A, Wu B, Aharonov A, D'Uva G, Bourke LM, Pitulescu ME, Chen H, de la Pompa JL, Shou W, Adams RH, Harten SK, Tzahor E, Zhou B, Harvey RP. Control of cardiac jelly dynamics by NOTCH1 and NRG1 defines the building plan for trabeculation. Nature. 2018;557:439–445. [PubMed: 29743679]
35. Goumans MJ, Valdimarsdottir G, Itoh S, Lebrin F, Larsson J, Mummery C, Karlsson S, ten Dijke P. Activin receptor-like kinase (ALK)1 is an antagonistic mediator of lateral TGFbeta/ALK5 signaling. Mol Cell. 2003;12:817–828. [PubMed: 14580334]
36. Leask Andrew. Getting to the heart of the matter: new insights into cardiac fibrosis. Circ Res. 2015;116:1269–1276. [PubMed: 25814687]
37. Muñoz-Félix JM, González-Núñez M, López-Novoa JM. ALK1-Smad1/5 signaling pathway in fibrosis development: friend or foe? Cytokine Growth Factor Rev. 2013;24:523–537. [PubMed: 24055043]
38. Anderson RH, Jensen B, Mohun TJ, Petersen SE, Aung N, Zemrak F, Planken RN, MacIver DH. Key Questions Relating to Left Ventricular Noncompaction Cardiomyopathy: Is the Emperor Still Wearing Any Clothes? Can J Cardiol. 2017;33:747–757. [PubMed: 28395867]
39. Sedaghat-Hamedani F, Haas J, Zhu J, Geier C, Kayvanpour E, Liss M, Lai A, Frese K, Pribe-Wolferts R, Amr A, Li DT, Samani OS, Carstensen A, Bordalo DM, Muller M, Fischer C, Shao J, Wang J, Nie M, Yuan L, Haßfeld S, Schwartz C, Zhou M, Zhou Z, Shu Y, Wang M, Huang K, Zeng Q, Cheng L, Fehlmann T, Ehlermann P, Keller A, Dieterich C, Streckfuß-Bomeke K, Liao Y, Gotthardt M, Katus HA, Meder B. Clinical genetics and outcome of left ventricular non-compaction cardiomyopathy. Eur Heart J. 2017;38:3449–3460. [PubMed: 29029073]
40. van Waning J, Moesker J, Heijsman D, Boersma E, Majoor-Krakauer D. Systematic Review of Genotype-Phenotype Correlations in Noncompaction Cardiomyopathy. J Am Heart Assoc. 2019;8:e012993. [PubMed: 31771441]
41. Luxán G, Casanova JC, Martínez-Poveda B, Prados B, D'Amato G, MacGrogan D, Gonzalez-Rajal A, Dobarro D, Torroja C, Martinez F, Izquierdo-García JL, Fernández-Friera L, Sabater-Molina M, Kong YY, Pizarro G, Ibañez B, Medrano C, García-Pavía P, Gimeno JR, Monserrat L, Jiménez-Borreguero LJ, de la Pompa JL. Mutations in the NOTCH pathway regulator MIB1 cause left ventricular noncompaction cardiomyopathy. Nat Med. 2013;19:193–201. [PubMed: 23314057]
42. DiMichele LA, Hakim ZS, Sayers RL, Rojas M, Schwartz RJ, Mack CP, Taylor JM. Transient expression of FRNK reveals stage-specific requirement for focal adhesion kinase activity in cardiac growth. Circ Res. 2009;104:1201–1208. [PubMed: 19372463]
43. Lin W, Li D, Cheng L, Li L, Liu F, Hand NJ, Epstein JA, Rader DJ. Zinc transporter Slc39a8 is essential for cardiac ventricular compaction. J Clin Invest. 2018;128:826–833. [PubMed: 29337306]
44. Lin W, Li D. Zinc and Zinc Transporters: Novel Regulators of Ventricular Myocardial Development. Pediatr Cardiol. 2018;39:1042–1051. [PubMed: 29536133]
45. Ali SK. Unique features of non-compaction of the ventricular myocardium in Arab and African patients. Cardiovasc J Afr. 2008;19:241–245. [PubMed: 18997984]
46. Gardner MM, Cohen MS. Clinical findings in right ventricular noncompaction in hypoplastic left heart syndrome. Congenit Heart Dis. 2017;12:783–786. [PubMed: 28643402]
47. Su T, Stanley G, Sinha R, D'Amato G, Das S, Rhee S, Chang AH, Poduri A, Raftrey B, Dinh TT, Roper WA, Li G, Quinn KE, Caron KM, Wu S, Miquerol L, Butcher EC, Weissman I, Quake

S, Red-Horse K. Single-cell analysis of early progenitor cells that build coronary arteries. Nature. 2018;559:356–362. [PubMed: 29973725]

48. Patro R, Duggal G, Love MI, Irizarry RA and Kingsford C. Salmon provides fast and bias-aware quantification of transcript expression. Nat Methods. 2017;14:417–419. [PubMed: 28263959]
49. Love MI, Huber W, Anders S. Moderated estimation of fold change and dispersion for RNA-seq data with DESeq2. Genome Biol. 2014;15:550. [PubMed: 25516281]
50. Zhu A, Ibrahim JG, Love MI. Heavy-tailed prior distributions for sequence count data: removing the noise and preserving large differences. Bioinformatics. 2019;35:2084–2092. [PubMed: 30395178]
51. Wu TB, Liang ZY, Zhang ZM, Liu CZ, Zhang LF, Gu YS, Peterson KL, Evans SM, Fu XD, Chen J. PRDM16 Is a Compact Myocardium-Enriched Transcription Factor Required to Maintain Compact Myocardial Cardiomyocyte Identity in Left Ventricle. Circulation. 2021.

NOVELTY AND SIGNIFICANCE

What Is known?

- ETS1 is the cause of congenital heart defects in Jacobsen syndrome (JBS).
- ETS1 is essential for vascular angiogenesis.
- The coronary vasculature is critical for the development of the ventricular compact zone during embryogenesis.
- Persistent extracellular matrix (ECM) synthesis enables enhanced trabecular growth in the trabecular layer.

What New Information Does This Article Contribute?

- Endothelial-specific deletion of ETS1 causes ventricular non-compaction, reproducing the phenotype arising from global deletion of ETS1
- Endothelial-specific deletion of ETS1 represses Alk1, Cldn5, Sox18, Robo4, Esm1 and Kdr, impairing coronary vascular development.
- Endothelial-specific deletion of ETS1 increases the expression of ECM genes through intensifying TGFBR2/TGFBR1/SMAD2 signaling pathway in the trabecular layer.

Dysfunction of the coronary endothelium and endocardium are associated with non-compaction cardiomyopathy. Our findings reveal that endothelial-specific deletion of the ETS1 transcription factor gene recapitulated the ventricular non-compaction phenotype observed in ETS1 gKO mice, along with impaired coronary vascular development and increased trabecular ECM expression. Our gene expression studies are consistent with and supportive of our *in vivo* studies, in which we identify six direct downstream target genes involved in angiogenesis that are regulated by ETS1 and demonstrate dysregulated TGFβ pathway signaling in the trabecular layer due to loss of ETS1 in endocardium. These data begin to identify a gene regulatory network involving ETS1 in ventricular and coronary vascular development. Specifically, our study identifies a non cell-autonomous mechanism by which loss of ETS1 leads to a differential effect on cardiomyocyte proliferation between the compact zone and trabecular layers underlying the development of ventricular non-compaction. These results have important implications not only for ventricular non-compaction, but also for hypoplastic left heart syndrome, which occurs at an unprecedented high frequency in JBS.

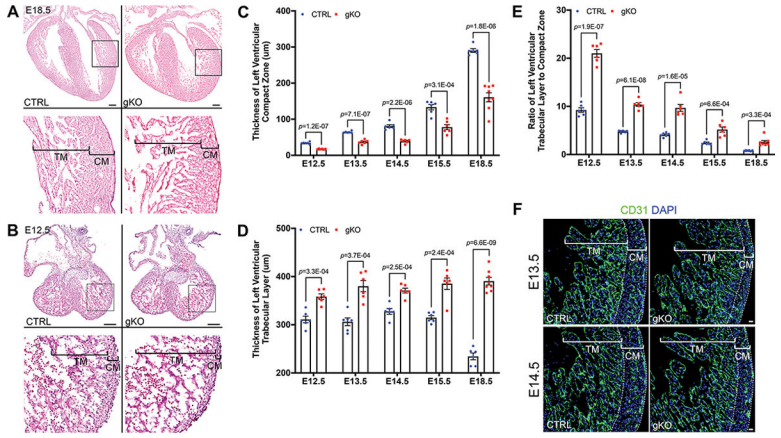

Figure 1. ETS1 global knockout causes ventricular non-compaction.

A and B, Representative images of heart sections stained with Hematoxylin and Eosin showing compact myocardium (CM) and trabecular myocardium (TM) in control and ETS1 global knockout (gKO) mice at (**A**) E18.5 and (**B**) E12.5. Scale bars: 200 μm. **C though E,** Graphs showing (**C**) compact myocardium thickness, (**D**) trabecular myocardium thickness and (**E**) ratio of trabecular myocardium thickness to compact myocardium thickness of left ventricles in control and gKO mice at different stages from E12.5 to E18.5 (CTRL, n=6; gKO, n=6 at each stage from E12.5 through E15.5, CTRL, n=6; gKO, n=8 at E18.5). **F,** Representative confocal images of CD31 immunofluorescence labeling endocardium in control and gKO mice at E13.5 and E14.5. Scale bars: 20 μm.

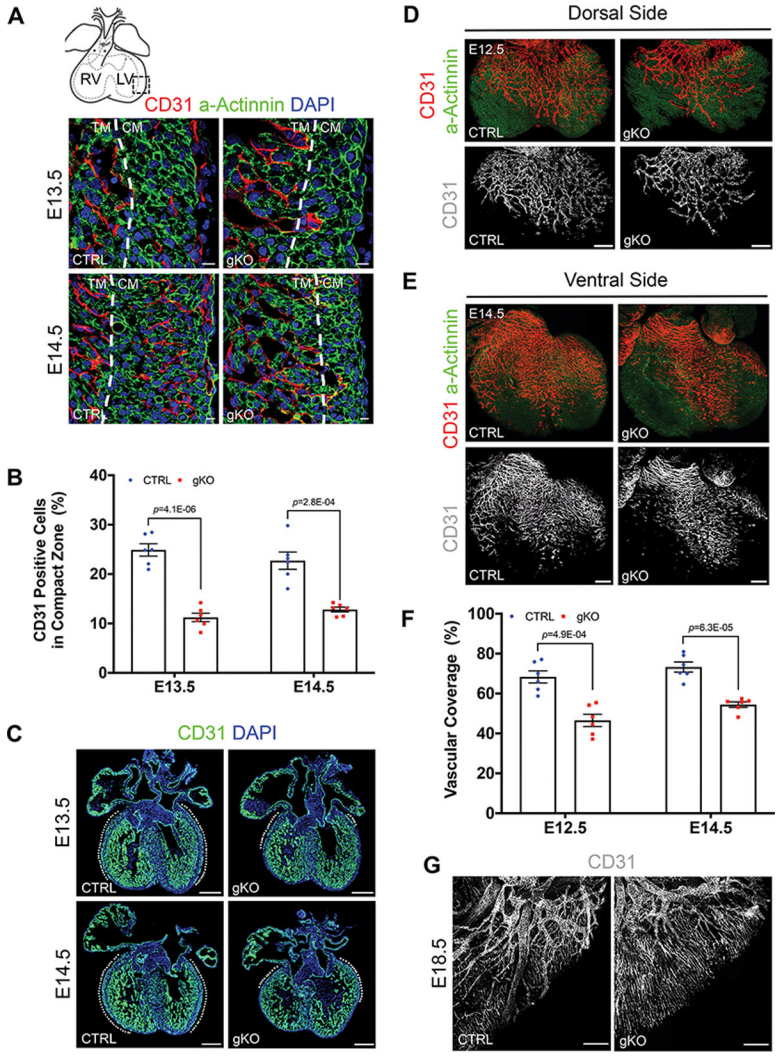

Figure 2. ETS1 global knockout causes coronary vascular defect.

A, Representative confocal images showing endothelial cells (red) in the compact zone in control and gKO mice at E13.5 and E14.5. Scale bars: 10 μm. **B,** Graph of quantitation of the percentage of CD31 positive cells in the compact zone in control and gKO mice at E13.5 and E14.5 (CTRL, n=6; gKO, n=6 at E13.5 and E14.5). **C,** Whole heart CD31 immunofluorescence images at E13.5 and E14.5 showing the endothelial cells in the compact zone in control and gKO mice. Scale bars: 200 μm. The white broken lines indicate the ventricular wall covered by coronary vasculature. **D and E,** Representative whole-mount confocal images showing the coronary vasculature (**D**) on the dorsal side of the heart at E12.5 and (**E**) on the ventral side of the heart at E14.5 in control and gKO mice. Scale bars: 200 μm. **F,** Graph of quantification of heart coverage on the dorsal side of the heart at E12.5 and on the ventral side of the heart at E14.5 in control and gKO mice. (CTRL, n=6; gKO, n=6 at E12.5 and E14.5). **G,** Representative whole-mount confocal images of the coronary vasculature at E18.5. Scale bars: 200 μm.

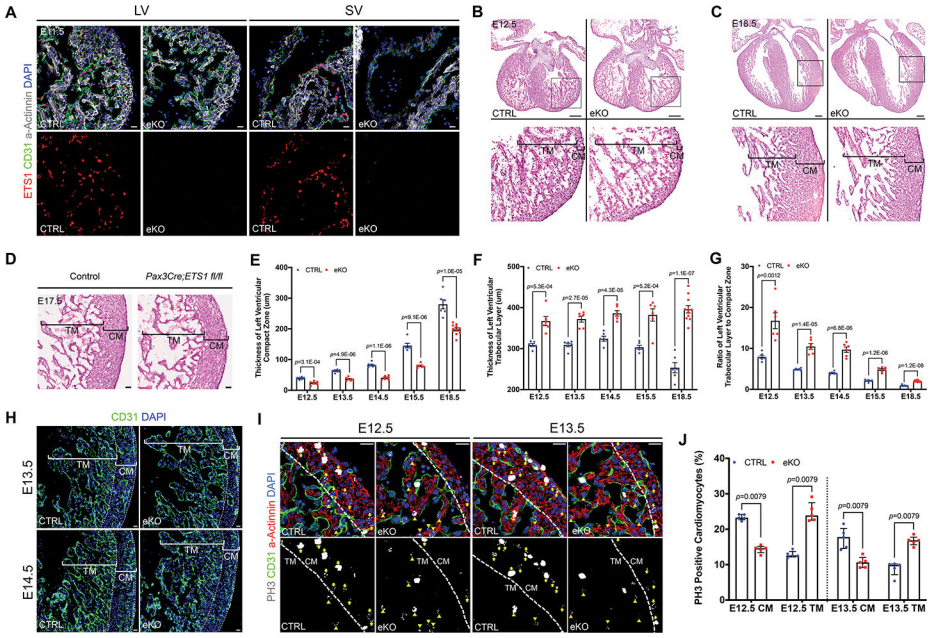

Figure 3. ETS1 endothelial deletion causes ventricular non-compaction.

A, ETS1 immunofluorescence showing ETS1 protein was undetectable in endocardium and sinus venosus (SV) endothelium in ETS1 endothelial conditional knockout (eKO) embryo. Scale bars: 20 μm. **B and C,** Representative images of heart sections stained with Hematoxylin and Eosin showing compact myocardium (CM) and trabecular myocardium (TM) in control and eKO mice at (**B**) E12.5 and (**C**) E18.5. Scale bars: 200 μm. **D,** Representative images of heart sections stained with Hematoxylin and Eosin showing compact myocardium and trabecular myocardium in control and neural crest cell conditional knockout mice at E17.5. Scale bars: 200 μm. **E though G,** Graphs showing (**E**) compact myocardium thickness, (**F**) trabecular myocardium thickness of left ventricles and (**G**) ratio of trabecular myocardium thickness to compact myocardium thickness in control and eKO mice at different stages from E12.5 to E18.5 (CTRL, n=6; eKO, n=6 at each stage from E12.5 through E15.5, CTRL, n=6; eKO, n=11 at E18.5). **H,** Representative confocal images of CD31 immunofluorescence labeling endocardium in control and eKO mice at E13.5 and E14.5. Scale bars: 20 μm. **I,** Representative confocal images of PH3 immunofluorescence showing proliferating cardiomyocytes in the compact zone (yellow arrowheads) and in the trabecular layer (yellow triangles) in control and eKO mice at E12.5 and E13.5. Scale bars: 20 μm. **J,** Graph of quantification of PH3 positive cardiomyocytes in compact myocardium (CM) and trabecular myocardium (TM) in control and eKO mice at E12.5 and E13.5. (CTRL, n=5; eKO, n=5).

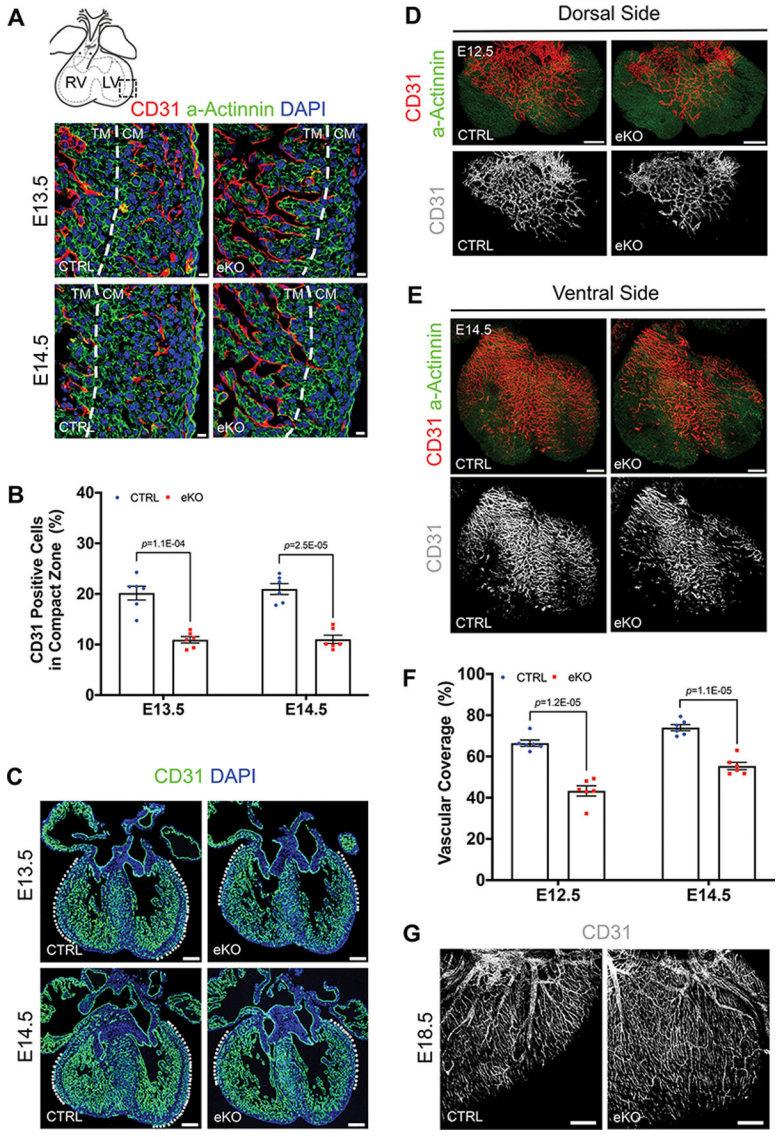

Figure 4. ETS1 endothelial deletion causes coronary vascular defect.

A, Representative confocal images showing endothelial cells (red) in the compact zone in control and eKO mice at E13.5 and E14.5. Scale bars: 10 μm. **B,** Graph of quantitation of the percentage of CD31 positive cells in the compact zone in control and eKO mice at E13.5 and E14.5 (CTRL, n=6; eKO, n=6 at E13.5 and E14.5). **C,** Whole heart CD31 immunofluorescence images at E13.5 and E14.5 showing the endothelial cells in the compact zone in control and gKO mice. **D and E,** Representative whole-mount confocal images showing the coronary vasculature (**D**) on the dorsal side of the heart at E12.5 and (**E**) on the ventral side of the heart at E14.5 in control and eKO mice. Scale bars: 200 μm. **F,** Graph of quantification of heart coverage on the dorsal side of the heart at E12.5 and on the ventral side of the heart at E14.5 in control and eKO mice. (CTRL, n=6; eKO, n=6 at E12.5 and E14.5). **G,** Representative whole-mount confocal images of the coronary vasculature at E18.5. Scale bars: 200 μm.

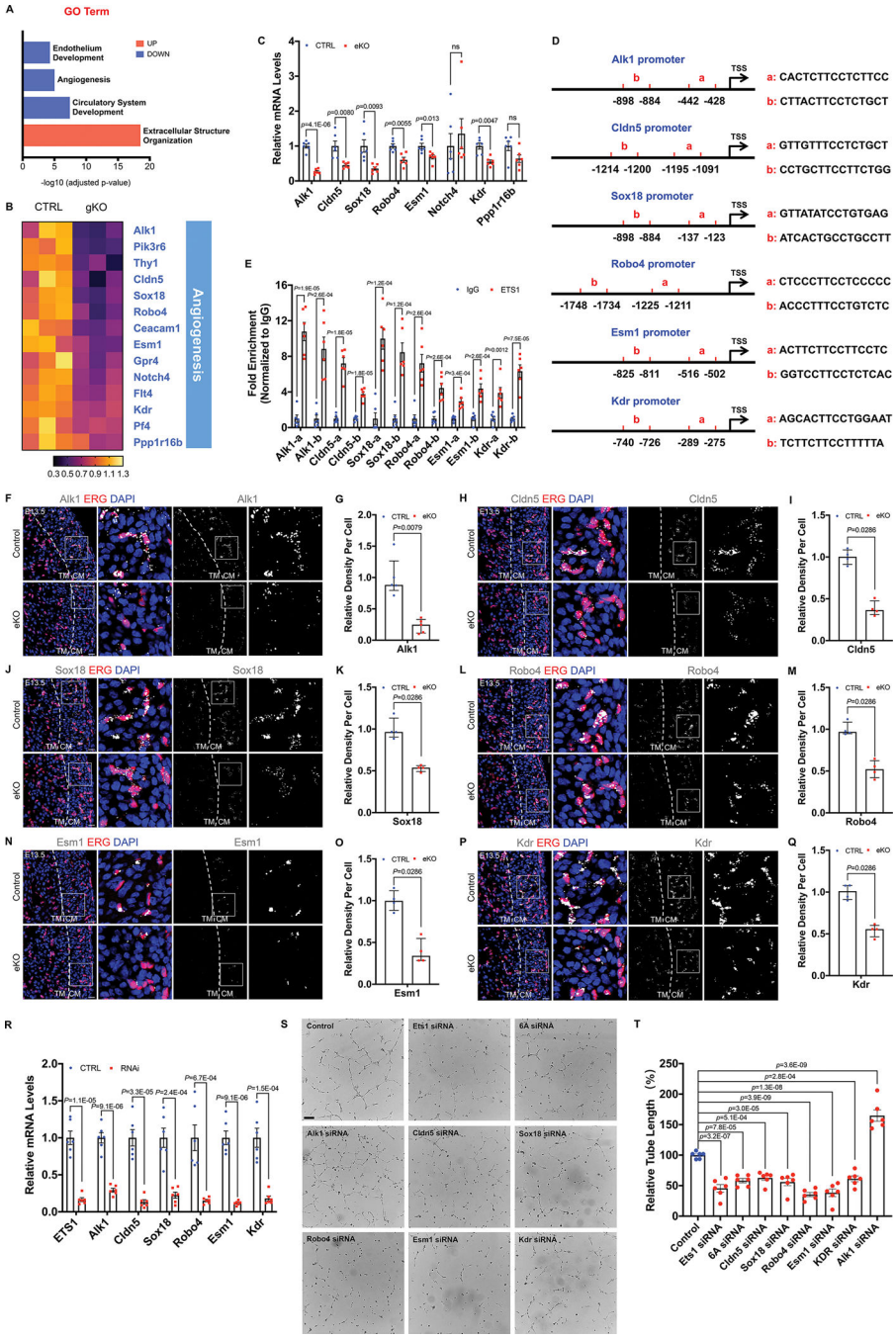

Figure 5. ETS1 endothelial deletion represses the levels of Alk1, Cldn5, Sox18, Robo4, Esm1 and Kdr.

A, Gene ontology (GO) enrichment analysis of differentially expressed genes by RNA sequencing (RNA-Seq). **B,** Heatmap of angiogenesis-relevant genes listed in descending order of magnitude in control and gKO mice at E12.5. Each column represents RNA-seq from an individual ventricle. (CTRL, n=3; gKO, n=3). **C,** Quantitative polymerase chain reaction (qPCR) analysis from E12.5 mouse ventricles showing the expression of the ETS1 target genes in control and eKO mice (CTRL, n=6; eKO, n=6). ns, not significant. **D,**

Potential binding sites of ETS1 in the promoter regions of Alk1, Cldn5, Sox18, Robo4, Esm1 and Kdr predicted by JASPAR (a and b, two potential ETS1 binding sites with the highest scores). **E,** ChIP-qPCR of ETS1 binding to the promoter region of Alk1, Cldn5, Sox18, Robo4, Esm1 and Kdr (ETS1, n=6; IgG, n=6). **F though Q,** Representative confocal images of RNAscope *in situ* hybridization of (**F**) Alk1, (**H**) Cldn5, (**J**) Sox18, (**L**) Robo4, (**N**) Esm1 and (**P**) Kdr, and quantification graph of signal intensity of (**G**) Alk1, (**I**) Cldn5, (**K**) Sox18, (**M**) Robo4, (**O**) Esm1 and (**Q**) Kdr in coronary endothelium showing the expression levels of these genes in control and eKO mouse heart at E13.5 (CTRL, n=5; eKO, n=5 for Alk1; CTRL, n=4; eKO, n=4 for Cldn5, Sox18, Robo4, Esm1 and Kdr). Scale bars: 20 μm. **R**, qPCR validation of the expression of ETS1, Alk1, Cldn5, Sox18, Robo4, Esm1 and Kdr after transfecting the siRNA in human coronary artery endothelial cells (HCAECs) respectively (CTRL, n=6; RNAi, n=6, respectively). **S and T,** Representative images (**S**) and quantitation graph (**T**) of tube formation of HCAECs after transfecting the siRNAs of ETS1, Alk1, Cldn5, Sox18, Robo4, Esm1 and Kdr individually or a cocktail of all six siRNAs (6A siRNA) for 48 hours. Images were taken six hours after seeding (CTRL, n=6; RNAi, n=6, respectively).

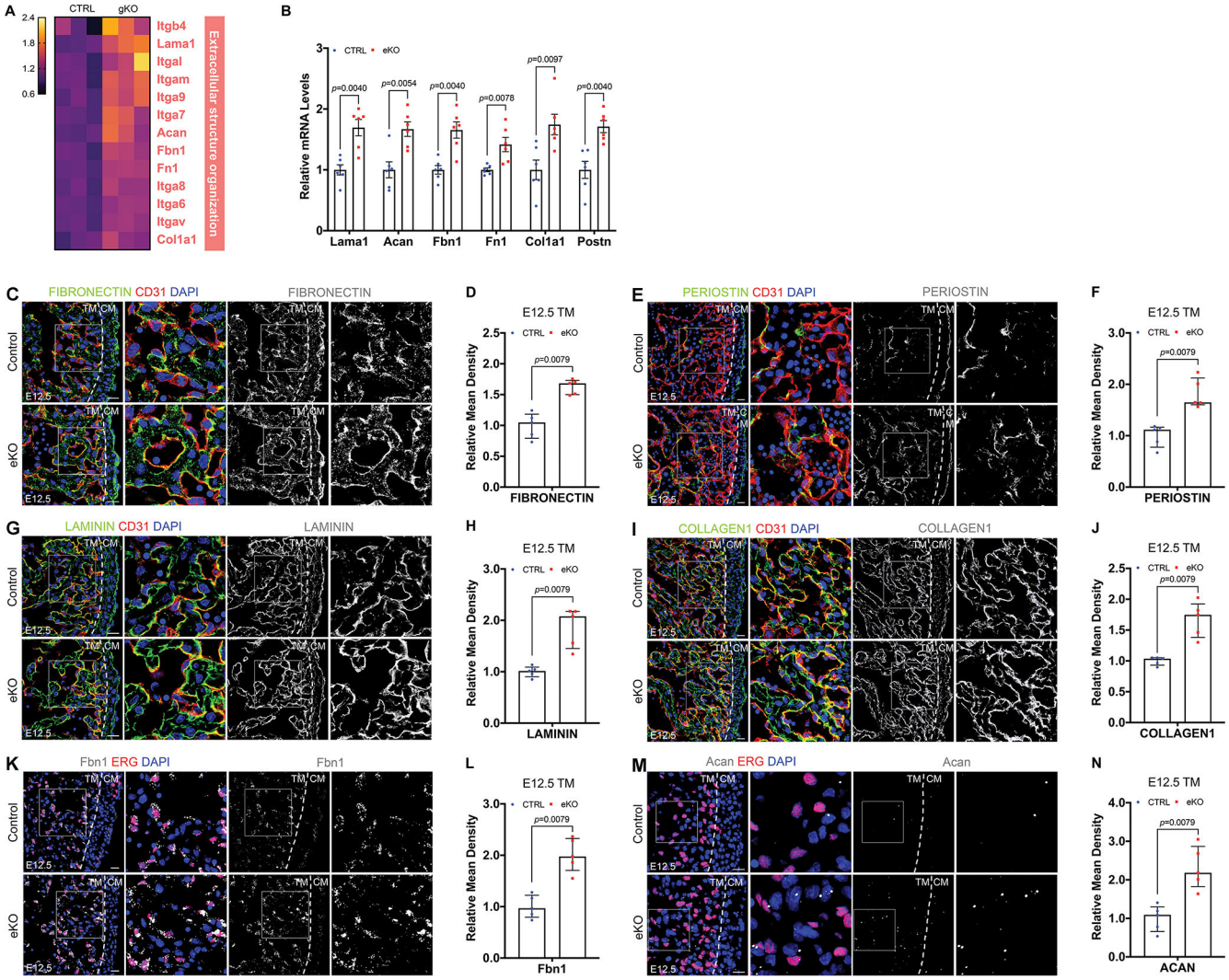

Figure 6. ETS1 endothelial deletion increases the expression of ECM genes in the trabecular layer.

A, Heatmap of genes relevant to extracellular structure organization in control and gKO mice at E12.5. Each column represents RNA-seq from an individual ventricle. (CTRL, n=3; gKO, n=3). **B,** Quantitative polymerase chain reaction analysis of ECM genes from E12.5 mouse ventricles (CTRL, n=6; eKO, n=6). **C though N,** Representative confocal images of immunofluorescence of (**C**) Fibronectin, (**E**) Periostin, (**G**) Laminin and (**I**) Collagen1 and RNAscope *in situ* hybridization of (**K**) Fbn1 and (**M**) Acan, and quantification graph of signal intensity of (**D**) Fibronectin, (**F**) Periostin, (**H**) Laminin, (**J**) Collagen1, (**L**) Fbn1 and (**N**) Acan in trabecular layer showing the expression levels and patterns of these ECM genes in control and eKO mouse heart at E12.5 (CTRL, n=5; eKO, n=5, respectively). Scale bars: 20 μm.

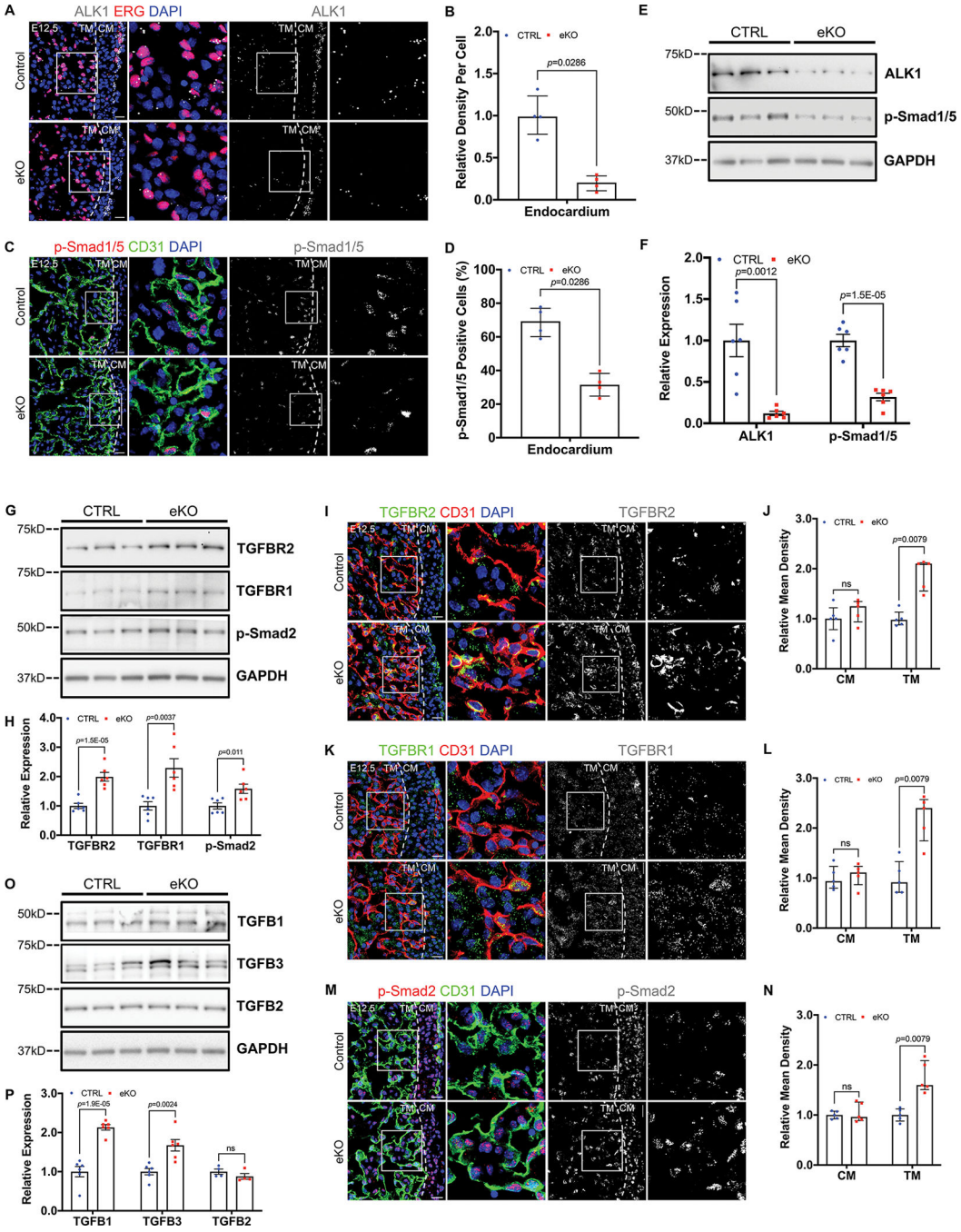

Figure 7. ETS1 endothelial deletion intensifies the TGFBR2/TGFBR1/SMAD2 signaling pathway.

A though D, Representative confocal images of immunofluorescence of (**A**) ALK1 and (**C**) p-Smad1/5 and quantitation graph of (**B**) ALK1 signal intensity and (**D**) percentage of p-Smad1/5 positive cells in endocardium showing their expression levels and patterns in control and eKO mouse heart at E12.5 (CTRL, n=4; eKO, n=4). Scale bars: 20 μm. **E and F,** (**E**) Western blot representative images and (**F**) Quantitation graph of ALK1 and p-Smad1/5 from E12.5 mouse ventricles in control and eKO mice (CTRL, n=6; eKO, n=6). **G and H,**

(**G**) Western blot representative images and (**H**) Quantitation graph of TGFBR2, TGFBR 1 and p-Smad2 from E12.5 mouse ventricles in control and eKO mice (CTRL, n=6; eKO, n=6). **I through N,** Representative confocal images of immunofluorescence of (**I**) TGFBR2, (**K**) TGFBR1 and (**M**) p-Smad2 and quantitation graph of signal intensity of (**J**) TGFBR2, (**L**) TGFBR1 and (**N**) p-Smad2 showing their expression levels and patterns in control and eKO mouse heart at E12.5 (CTRL, n=5; eKO, n=5). Scale bars: 20 μm. ns, not significant. **O and P,** (**O**) Western blot representative images and (**P**) quantitation graph of TGFB1, TGFB3 and TGFB2 from E12.5 mouse ventricles in control and eKO mice (CTRL, n=6; eKO, n=6 for TGFB1 and TGFB3, CTRL, n=4; eKO, n=4 for TGFB2). ns, not significant.

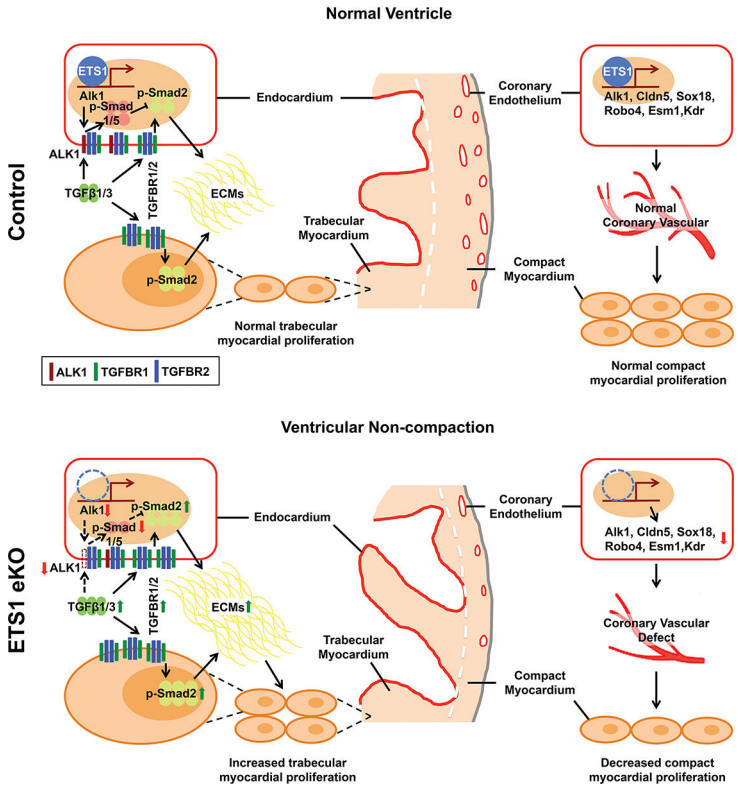

Figure 8. Model of the role of ETS1 for ventricular non-compaction.

Endothelial-specific deletion of ETS1 significantly represses the levels of Alk1, Cldn5, Sox18, Robo4, Esm1 and Kdr, six direct targets of ETS1 in endothelial cells, resulting in a coronary vascular defect and in association with decreased cardiomyocyte proliferation in the compact zone. Down-regulated ALK1 expression by the loss of ETS1 in the endocardium, along with the up-regulation of TGFβ1 and TGFβ3, amplifies the TGFBR2/TGFBR1/SMAD2 signaling pathway and increases ECM expression in the trabecular layer, coinciding with increased trabecular cardiomyocyte proliferation. Together, loss of ETS1 in endothelial cells causes ventricular non-compaction.